

## Electronic Supplementary Information

### **Carbon–Sulfur Bond Reductive Coupling from a Platinum(II) Thiolate Complex**

*Maryam Niazi,<sup>a</sup> Hamid R. Shahsavari,<sup>a\*</sup> Mohsen Golbon Haghighi,<sup>b</sup> Mohammad Reza Halvagar,<sup>c</sup> Samaneh Hatami<sup>a</sup> and Behrouz Notash<sup>b</sup>*

<sup>a</sup>Department of Chemistry, Institute for Advanced Studies in Basic Sciences (IASBS), Yousef Sobouti Blvd., Zanzan 45137-6731, Iran.

<sup>b</sup>Department of Chemistry, Shahid Beheshti University, Evin, Tehran 19839-69411, Iran

<sup>c</sup>Chemistry & Chemical Engineering Research Center of Iran, Tehran, 14968-13151, Iran

Email: [shahsavari@iasbs.ac.ir](mailto:shahsavari@iasbs.ac.ir)

Contents:	Page
<b>Figure S1.</b> Reaction of complex <b>1a</b> with 3eq of MeI as monitored by $^1\text{H}$ NMR spectroscopy in $\text{CD}_2\text{Cl}_2$ at room temperature. (I) Aromatic region. (II) Aliphatic region. (a) Pure complex <b>1a</b> , (b) immediately after addition of MeI, (c) 5 min (d) 15 min, (e) 30 min, (f) 60 min, (g) 120 min, (h) 180 min, (i) 240 min (j) 480 min and (k) pure complex <b>2a</b> . The signal assignments are shown.	3
<b>Figure S2.</b> $^1\text{H}$ NMR spectra of reaction mixture of complex <b>1a</b> with (a) $\text{CD}_3\text{I}$ and (b) MeI in $\text{CD}_2\text{Cl}_2$ at room temperature.	4
<b>Figure S3.</b> Reaction of complex <b>1a</b> with excess MeI as monitored by $^{31}\text{P}$ $\{^1\text{H}\}$ NMR spectroscopy in $\text{CD}_2\text{Cl}_2$ at low temperature (223 K). (a) Pure complex <b>1a</b> , (b) immediately after addition of MeI and (c) after 15 min. The signal assignments are shown.	5
<b>Scheme S1.</b> Suggested possible routes for reaction of methyl iodide with complex <b>1a</b> .	6
<b>Figure S4.</b> Reaction of complex <b>1b</b> with 3eq of MeI as monitored by $^{31}\text{P}$ $\{^1\text{H}\}$ NMR spectroscopy in $\text{CD}_2\text{Cl}_2$ at room temperature. (a) Pure complex <b>1b</b> , (b) immediately after addition of MeI, (c) 15 min (d) 30 min, (e) 45 min, (f) 60 min, (g) 75 min, (h) 90 min, (i) 105 min and (j) 120 min and (k) 240 min. The signal assignments are shown.	7
<b>Figure S5.</b> Reaction of complex <b>1b</b> with 3eq of MeI as monitored by $^1\text{H}$ NMR spectroscopy in $\text{CD}_2\text{Cl}_2$ at room temperature. (I) Aromatic region. (II) Aliphatic region. (a) Pure complex <b>1b</b> , (b) immediately after addition of MeI, (c) 15 min (d) 30 min, (e) 45 min, (f) 60 min, (g) 75 min, (h) 90 min, (i) 105 min and (j) 120 min, (k) 240 min and (l) pure complex <b>2a</b> . The signal assignments are shown.	8
<b>Table S1.</b> Crystallographic and structure refinement data for <b>A</b> , <b>2a</b> , <b>2b</b> and <b>3-PF<sub>6</sub></b> .	9
<b>Table S2.</b> Selected Distances [ $\text{\AA}$ ] and Angles [ $^\circ$ ] for complexes <b>A</b> , <b>2a</b> and <b>2b</b> .	10
<b>Figure S6.</b> Representations of the X-ray crystal structures of complexes (a) $[\text{Pt}(\text{ppy})(\text{PPh}_3)\text{Cl}]$ , <b>A</b> , (b) $[\text{Pt}(\text{ppy})(\text{PPh}_3)\text{I}]$ , <b>2a</b> , and (c) $[\text{Pt}(\text{ppy})(\text{PPh}_3)\text{Br}]$ , <b>2b</b> , showing all non-hydrogen atoms as 40% thermal ellipsoids.	11
<b>Figure S7.</b> $\text{C-H}\cdots\pi$ interaction between the $\text{C-H}$ group adjacent to metalated carbon atom of ppy ligand and the phenyl ring of $\text{PPh}_3$ ligand in complexes (a) <b>A</b> , (b) <b>2a</b> , (c) <b>2b</b> and (d) <b>3-PF<sub>6</sub></b> (green lines).	12
<b>Figure S8.</b> $\text{C-H}\cdots\text{X}$ interaction between the $\text{C-H}$ group adjacent to coordinated nitrogen atom of ppy ligand and the coordinated halogen ligand in complexes (a) <b>A</b> , (b) <b>2a</b> and (c) <b>2b</b> (green lines).	13
<b>Figure S9.</b> $^1\text{H}$ NMR spectra of $[\text{Pt}(\text{ppy})(\text{PPh}_3)\text{X}]$ , $\text{X} = \text{Cl}, \text{Br}$ and $\text{I}$ , in $\text{CDCl}_3$ , illustrating the effect of the halide ligand on the chemical shift of hydrogen adjacent to the coordinated nitrogen atom.	14
<b>Figure S10.</b> Weak intramolecular $\pi\cdots\pi$ contact between the $\text{Spy}$ and phenyl ring of $\text{PPh}_3$ in complex <b>3-PF<sub>6</sub></b> .	15
<b>Figure S11.</b> Crystal packing of complexes (a) <b>A</b> and (b) <b>2b</b> are displaying the intermolecular contacts. The supramolecular packing is formed by dimers supported by intermolecular $\pi\cdots\pi$ interactions involving two ppy ligands.	16
<b>Figure S12.</b> Partial view of the 2D-network of complex <b>2b</b> in the solid state. The hydrogen atoms are omitted for clarity, except for the hydrogen atoms being involved in Hydrogen bonding.	17
<b>Figure S13.</b> All possible geometries for complex <b>1a</b> .	18

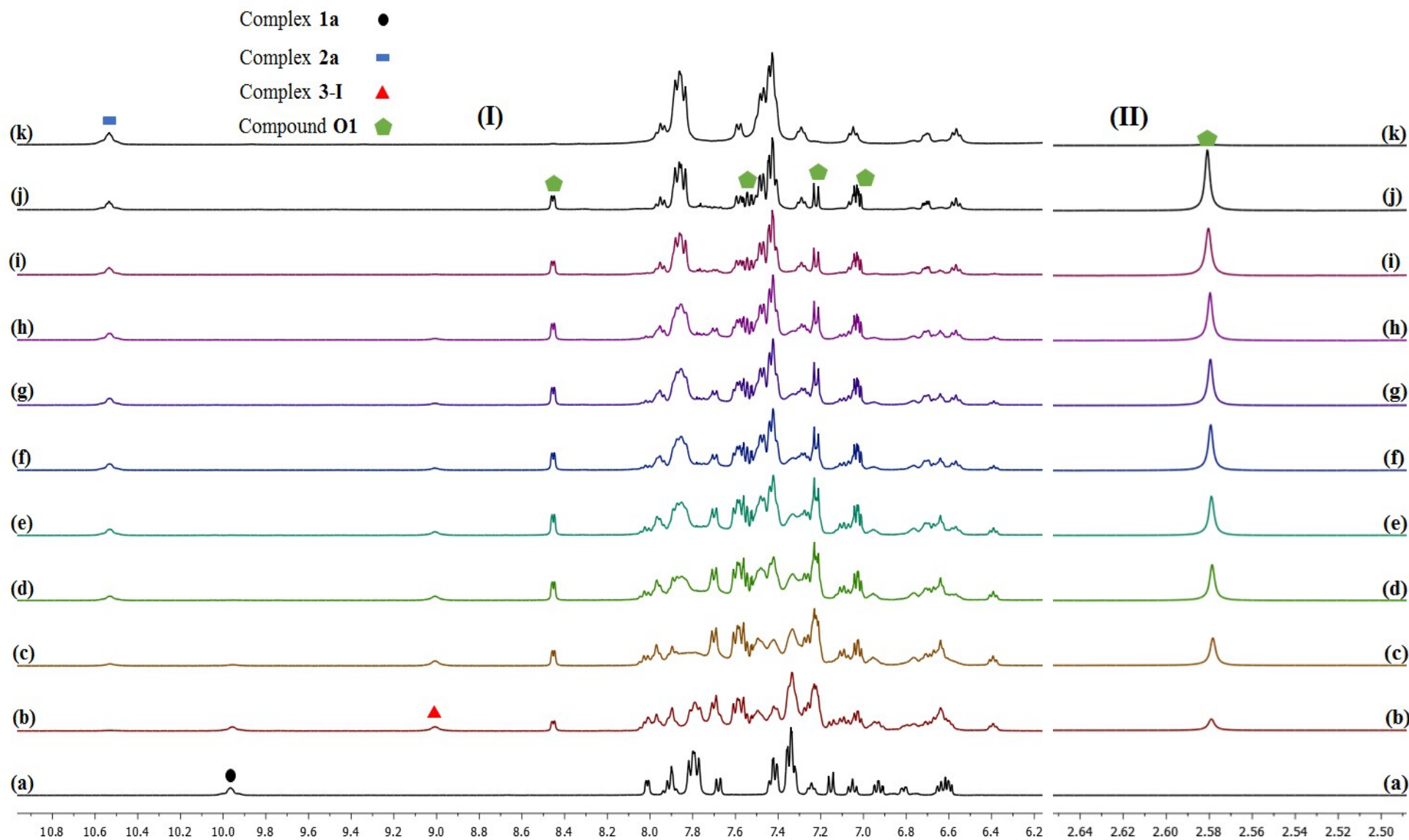


**Figure S1.** Reaction of complex **1a** with 3eq of MeI as monitored by  $^1\text{H}$  NMR spectroscopy in  $\text{CD}_2\text{Cl}_2$  at room temperature. (I) Aromatic region. (II) Aliphatic region. (a) Pure complex **1a**, (b) immediately after addition of MeI, (c) 5 min (d) 15 min, (e) 30 min, (f) 60 min, (g) 120 min, (h) 180 min, (i) 240 min (j) 480 min and (k) pure complex **2a**. The signal assignments are shown.

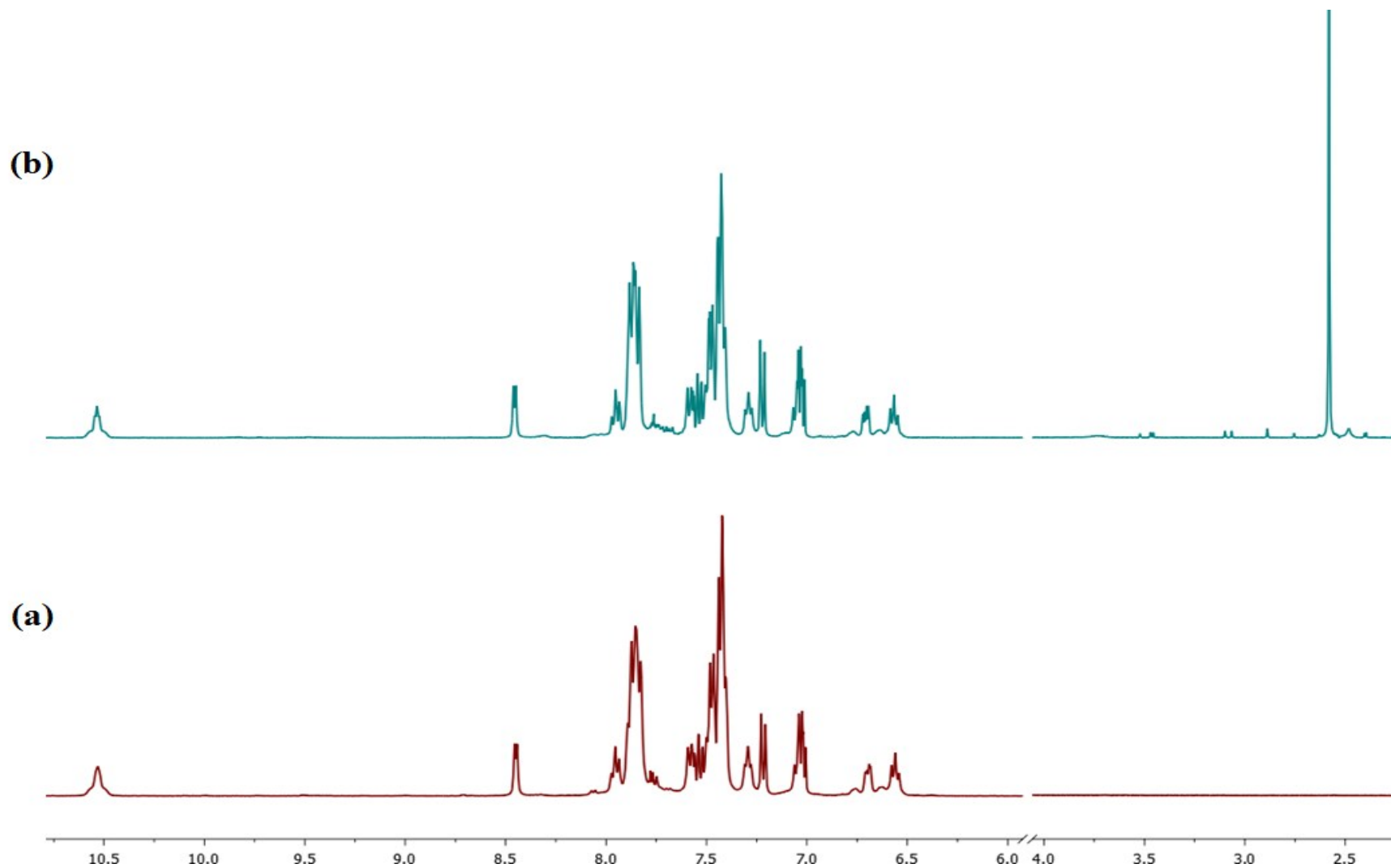


**Figure S2.**  $^1\text{H}$  NMR spectra of reaction mixture of complex **1a** with (a)  $\text{CD}_3\text{I}$  and (b)  $\text{MeI}$  in  $\text{CD}_2\text{Cl}_2$  at room temperature.

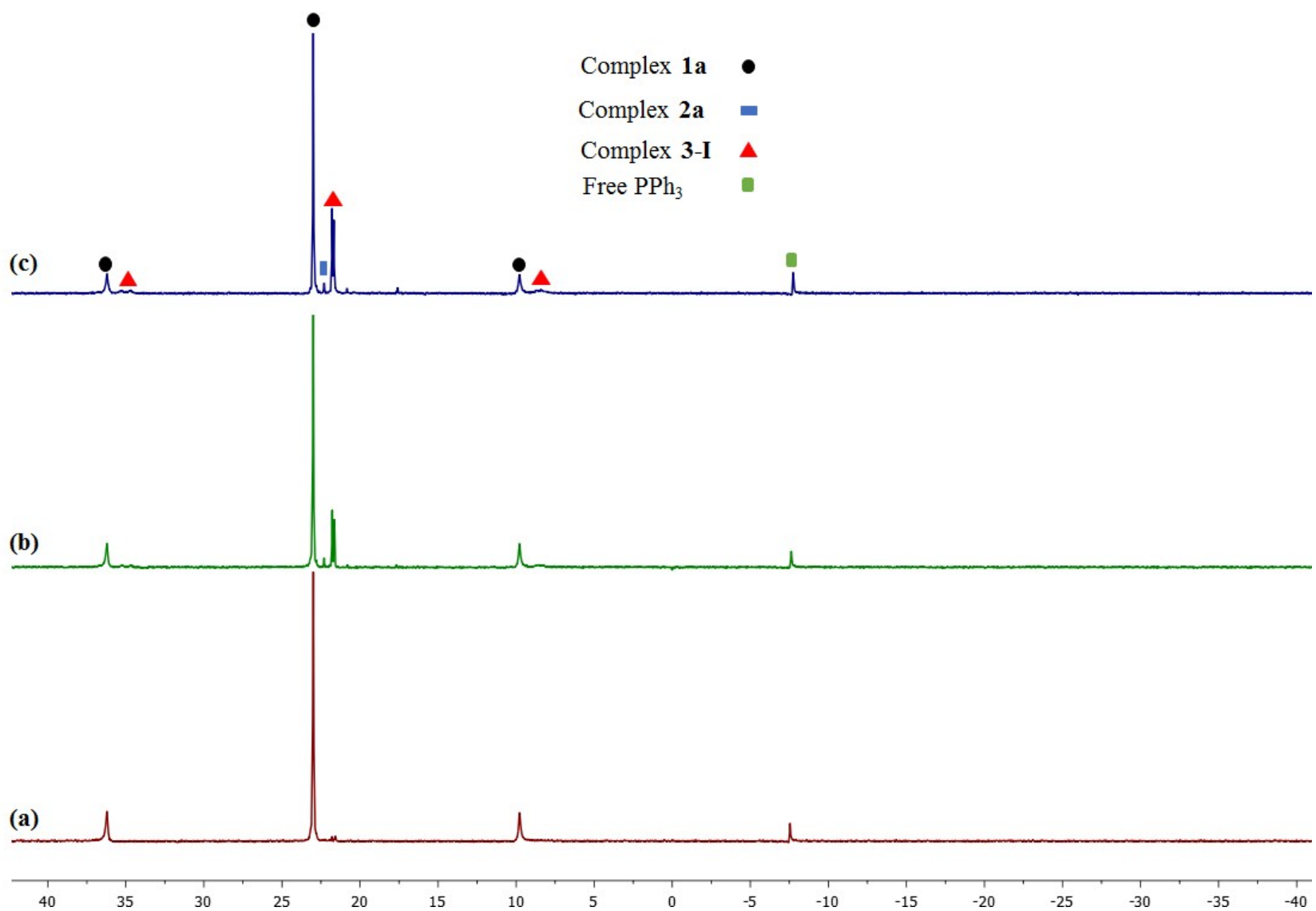
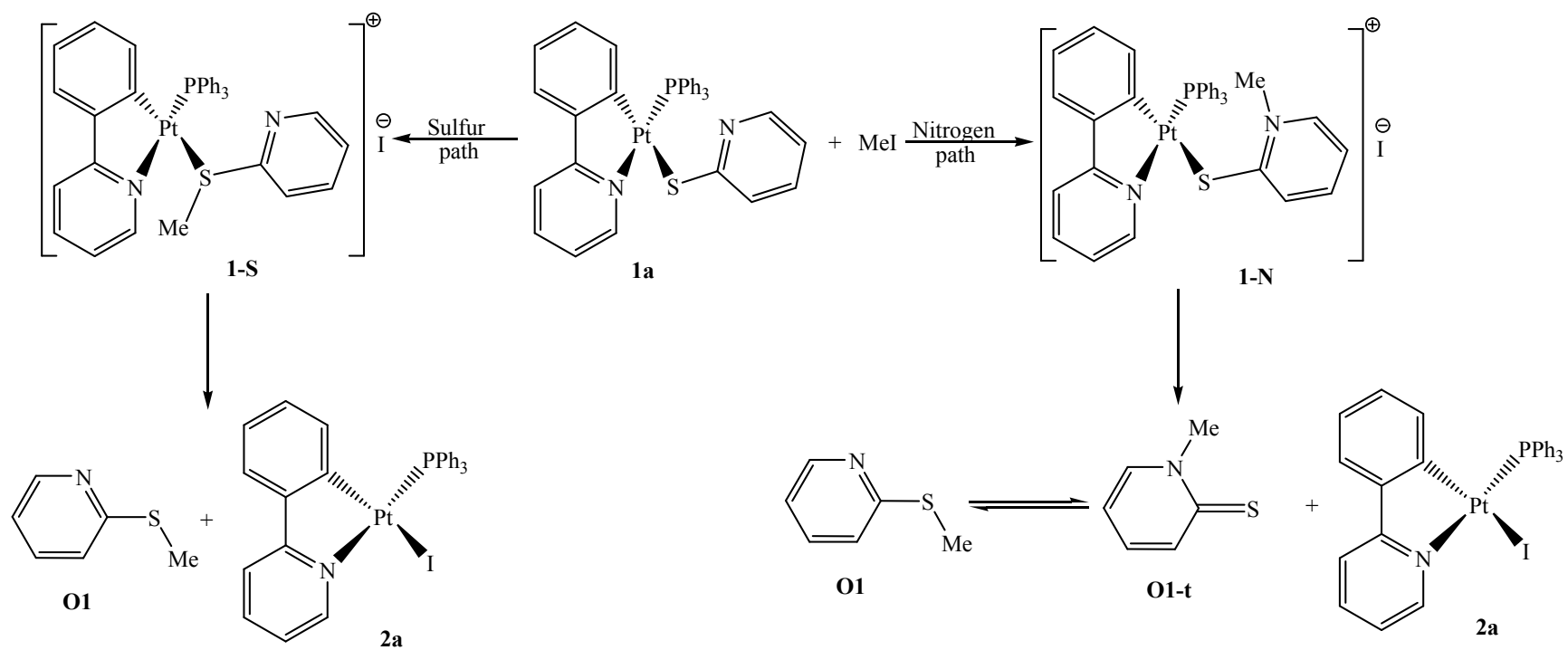


**Figure S3.** Reaction of complex **1a** with excess MeI as monitored by  $^{31}\text{P} \{^1\text{H}\}$  NMR spectroscopy in  $\text{CD}_2\text{Cl}_2$  at low temperature (223 K). (a) Pure complex **1a**, (b) immediately after addition of MeI and (c) after 15 min. The signal assignments are shown.



**Scheme S1.** Suggested possible routes for reaction of methyl iodide with complex **1a**.

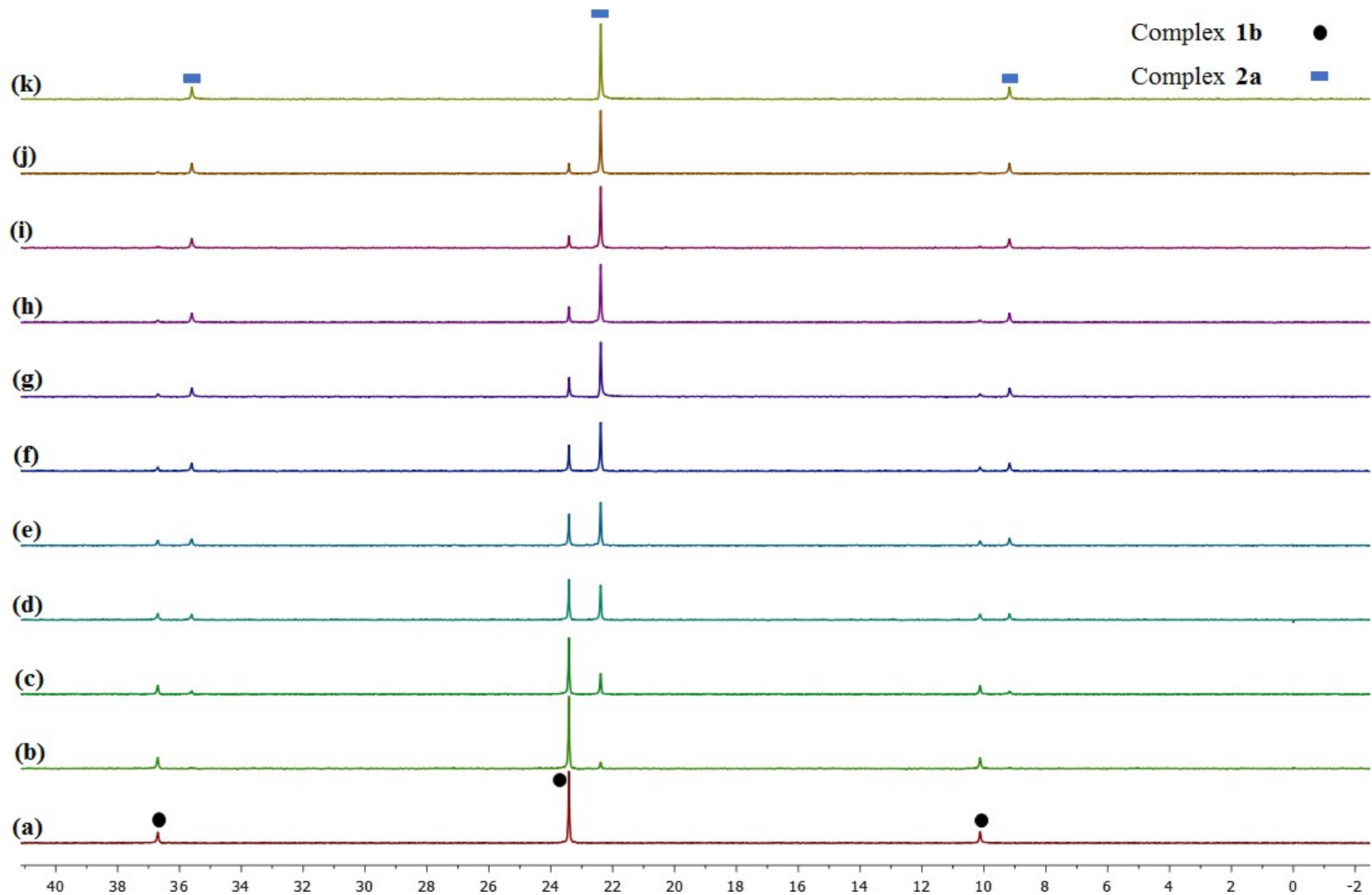


**Figure S4.** Reaction of complex **1b** with 3eq of MeI as monitored by  $^{31}\text{P}$   $\{^1\text{H}\}$  NMR spectroscopy in  $\text{CD}_2\text{Cl}_2$  at room temperature. (a) Pure complex **1b**, (b) immediately after addition of MeI, (c) 15 min (d) 30 min, (e) 45 min, (f) 60 min, (g) 75 min, (h) 90 min, (i) 105 min and (j) 120 min and (k) 240 min. The signal assignments are shown.

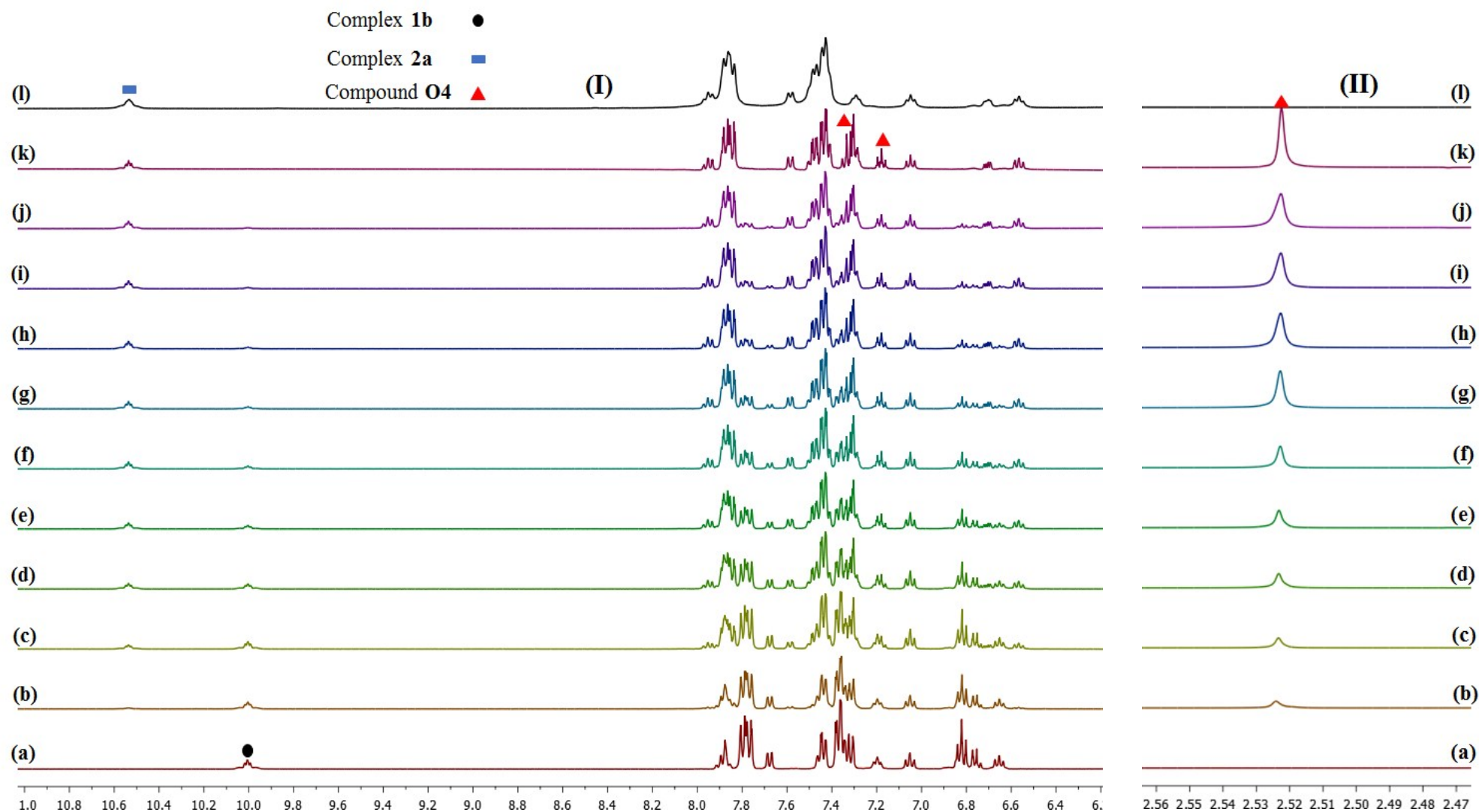


**Figure S5.** Reaction of complex **1b** with 3eq of MeI as monitored by  $^1\text{H}$  NMR spectroscopy in  $\text{CD}_2\text{Cl}_2$  at room temperature. (I) Aromatic region. (II) Aliphatic region. (a) Pure complex **1b**, (b) immediately after addition of MeI, (c) 15 min (d) 30 min, (e) 45 min, (f) 60 min, (g) 75 min, (h) 90 min, (i) 105 min and (j) 120 min, (k) 240 min and (l) pure complex **2a**. The signal assignments are shown.

**Table S1.** Crystallographic and structure refinement data for **A**, **2a**, **2b** and **3-PF<sub>6</sub>**.

	<b>A</b>	<b>2a</b>	<b>3b</b>	<b>3-PF<sub>6</sub></b>
Formula	C <sub>29</sub> H <sub>23</sub> ClNPt	C <sub>29</sub> H <sub>27</sub> INO <sub>2</sub> Pt	C <sub>29</sub> H <sub>23</sub> BrNPt	C <sub>64</sub> H <sub>52</sub> Cl <sub>2</sub> F <sub>6</sub> N <sub>3</sub> P <sub>3</sub> Pt <sub>2</sub> S
Formula weight	646.8	774.48	691.43	1563.12
T (K)	293(2)	298(2)	293(2)	298(2)
λ (Å)	0.71073	0.71073	0.71073	0.71073
Crystal system	Triclinic	Monoclinic	Triclinic	Monoclinic
Space Group	<i>P</i> $\bar{1}$	<i>P</i> 2 <sub>1</sub> / <i>c</i>	<i>P</i> $\bar{1}$	<i>P</i> 2 <sub>1</sub> / <i>n</i>
Crystal size(mm)	0.30×0.20×0.15	0.20×0.15×0.05	0.15×0.08×0.05	0.45×0.10×0.05
<i>a</i> (Å)	9.969(2)	17.402(4)	9.995(2)	20.818(4)
<i>b</i> (Å)	10.317(2)	9.3857(19)	10.493(2)	10.720(2)
<i>c</i> (Å)	13.607(3)	17.827(4)	13.571(3)	27.890(6)
α (°)	79.10(3)	90	79.34(3)	90
β (°)	70.81(3)	111.51(3)	70.61(3)	98.70(3)
γ (°)	68.00(3)	90	68.37(3)	90
<i>V</i> (Å <sup>3</sup> )	1222.0(5)	2709.1(9)	1244.8(4)	6153(2)
<i>Z</i>	2	4	2	4
<i>D</i> <sub>calc</sub> (g cm <sup>-3</sup> )	1.758	1.899	1.845	1.688
θ <sub>min</sub> , θ <sub>max</sub> (°)	3.1-26.9	2.49-25.00	2.09-25.00	2.14-25.00
<i>F</i> <sub>000</sub>	628	1480	664	3048
μ (mm <sup>-1</sup> )	5.934	6.404	7.323	4.802
Index ranges	-11 ≤ <i>h</i> ≤ 12 -12 ≤ <i>k</i> ≤ 13 -17 ≤ <i>l</i> ≤ 17	-20 ≤ <i>h</i> ≤ 20 -11 ≤ <i>k</i> ≤ 10 -17 ≤ <i>l</i> ≤ 21	-11 ≤ <i>h</i> ≤ 11 -12 ≤ <i>k</i> ≤ 12 -16 ≤ <i>l</i> ≤ 16	-24 ≤ <i>h</i> ≤ 24 -12 ≤ <i>k</i> ≤ 12 -33 ≤ <i>l</i> ≤ 33
Data collected	9831	12006	9090	32663
Unique data	4977	4763	4350	10828
<i>R</i> <sub><i>I</i></sub> <sup>a</sup> , <i>wR</i> <sub>2</sub> <sup>b</sup> ( <i>I</i> > 2σ( <i>I</i> ))	0.0379, 0.0786	0.0808, 0.1491	0.0849, 0.1622	0.0609, 0.1050
<i>R</i> <sub><i>I</i></sub> <sup>a</sup> , <i>wR</i> <sub>2</sub> <sup>b</sup> (all data)	0.0519, 0.0763	0.1747, 0.1745	0.1881, 0.1881	0.1467, 0.1221
GOF on <i>F</i> <sup>2</sup> (S)	1.002	0.890	0.876	0.803
CCDC No.	1457812	1457810	1457809	1496283

$$^a R_1 = \frac{\sum ||F_o| - |F_c||}{\sum |F_o|}, \quad ^b wR_2 = \left[ \frac{\sum (w(F_o^5 - F_c^2)^2)}{\sum w(F_o^2)^2} \right]^{1/2}$$

**Table S2.** Selected Distances [Å] and Angles [°] for complexes **A**, **2a** and **2b**.

	<b>A</b> (X1 = Cl1)	<b>2a</b> (X1 = I1)	<b>2b</b> (X = Br1)
Pt1-C1	2.002(8)	2.04(2)	1.98(3)
Pt1-N1	2.101(7)	2.126(18)	2.15(3)
Pt1-P1	2.2288(18)	2.225(6)	2.210(7)
Pt1-X1	2.373(3)	2.6672(19)	2.491(3)
C1-Pt1-N1	80.1(3)	79.3(9)	78.7(13)
C1-Pt1-P1	95.7(2)	95.5(7)	96.2(10)
C1-Pt1-X1	172.6(2)	165.2(7)	172.1(10)
N1-Pt1-P1	175.2(2)	174.5(5)	174.9(9)
N1-Pt1-X1	92.5(2)	92.8(5)	93.8(8)
P1-Pt1-X1	91.67(8)	92.73(15)	91.34(19)

---

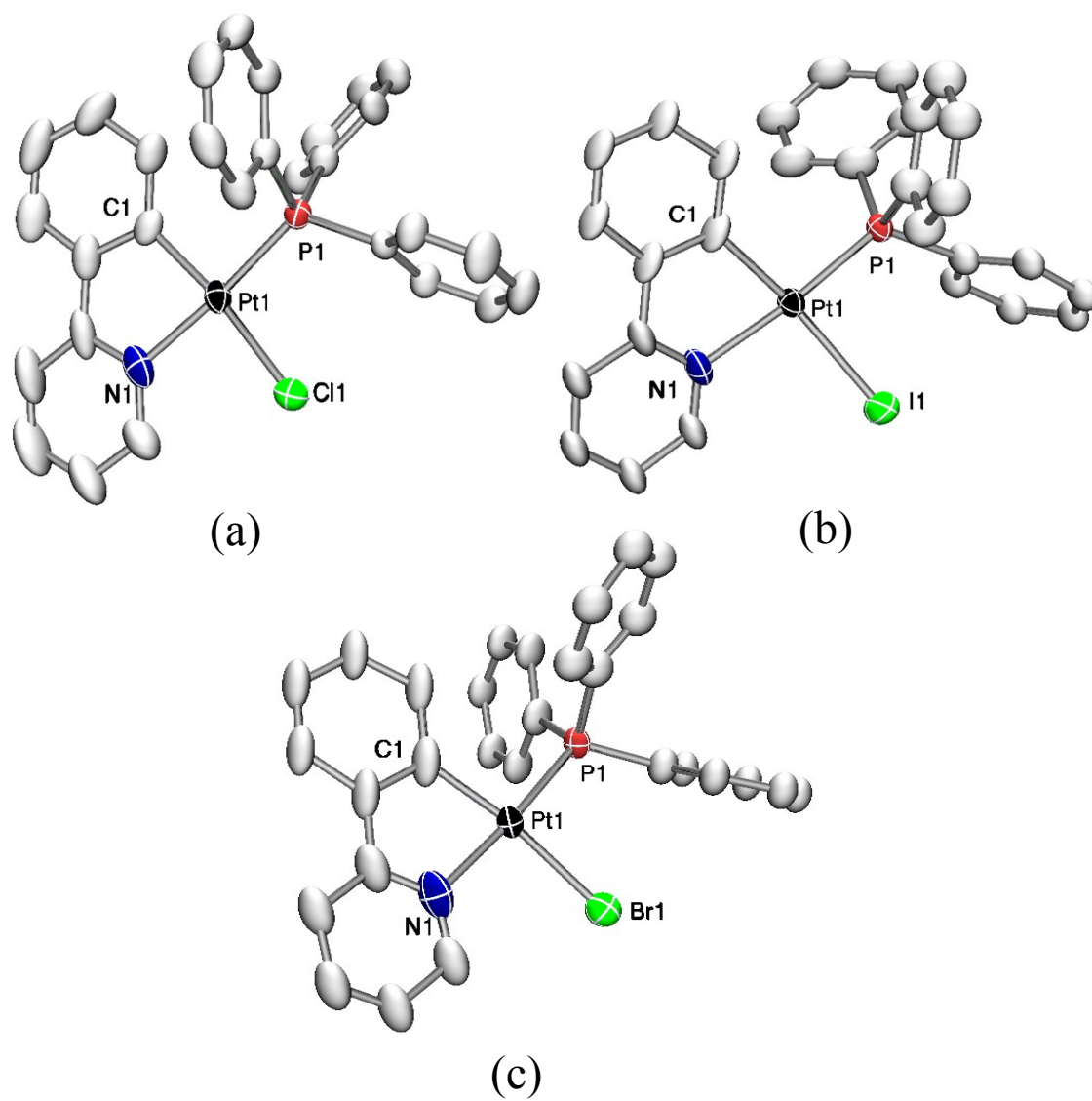


**Figure S6.** Representations of the X-ray crystal structures of complexes (a) [Pt(ppy)(PPh<sub>3</sub>)Cl], **A**, (b) [Pt(ppy)(PPh<sub>3</sub>)I], **2a**, and (c) [Pt(ppy)(PPh<sub>3</sub>)Br], **2b**, showing all non-hydrogen atoms as 40% thermal ellipsoids.

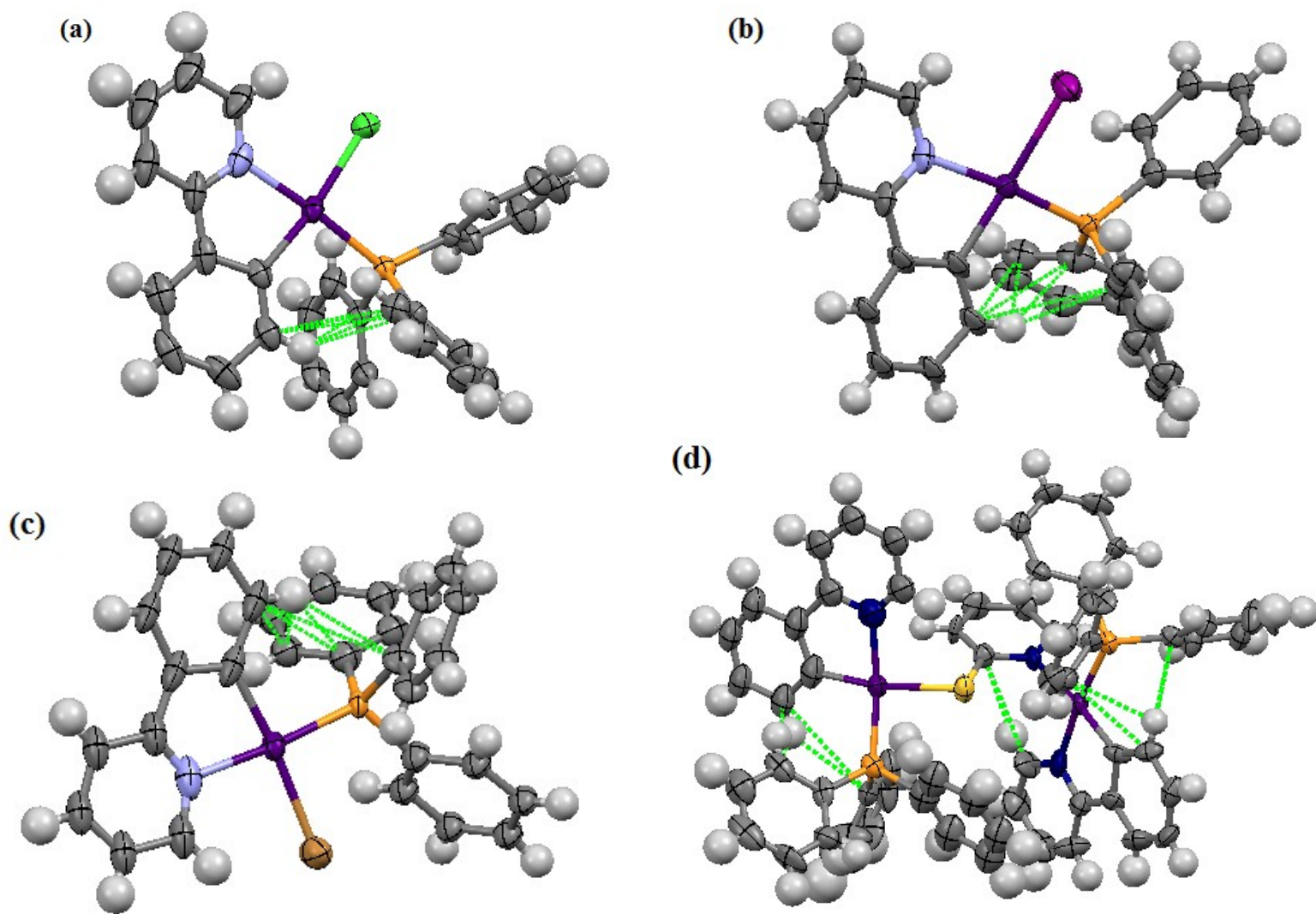


**Figure S7.** C-H... $\pi$  interaction between the C-H group adjacent to metalated carbon atom of ppy ligand and the phenyl ring of PPh<sub>3</sub> ligand in complexes (a) **A**, (b) **2a**, (c) **2b** and (d) **3-PF<sub>6</sub>** (green lines).

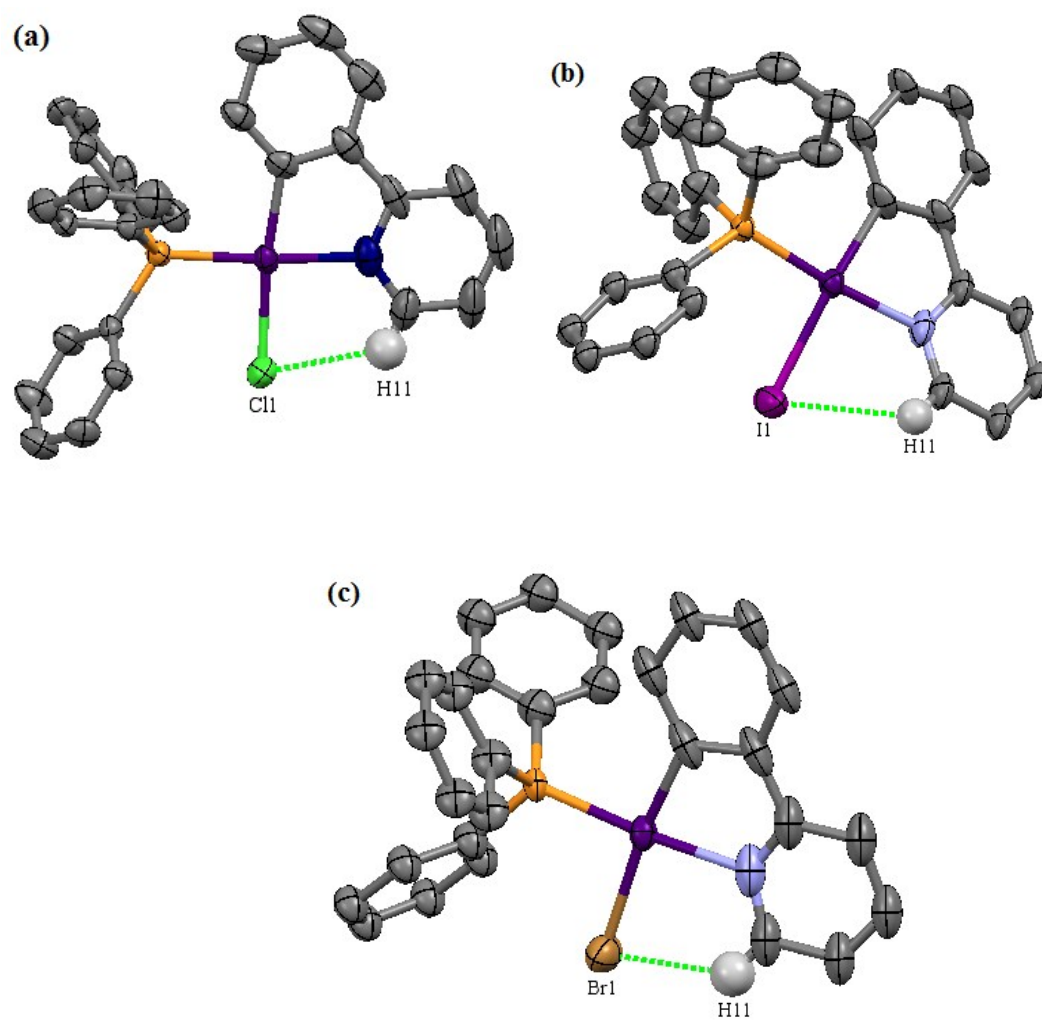


**Figure S8.** C–H···X interaction between the C–H group adjacent to coordinated nitrogen atom of ppy ligand and the coordinated halogen ligand in complexes (a) **A**, (b) **2a** and (c) **2b** (green lines).

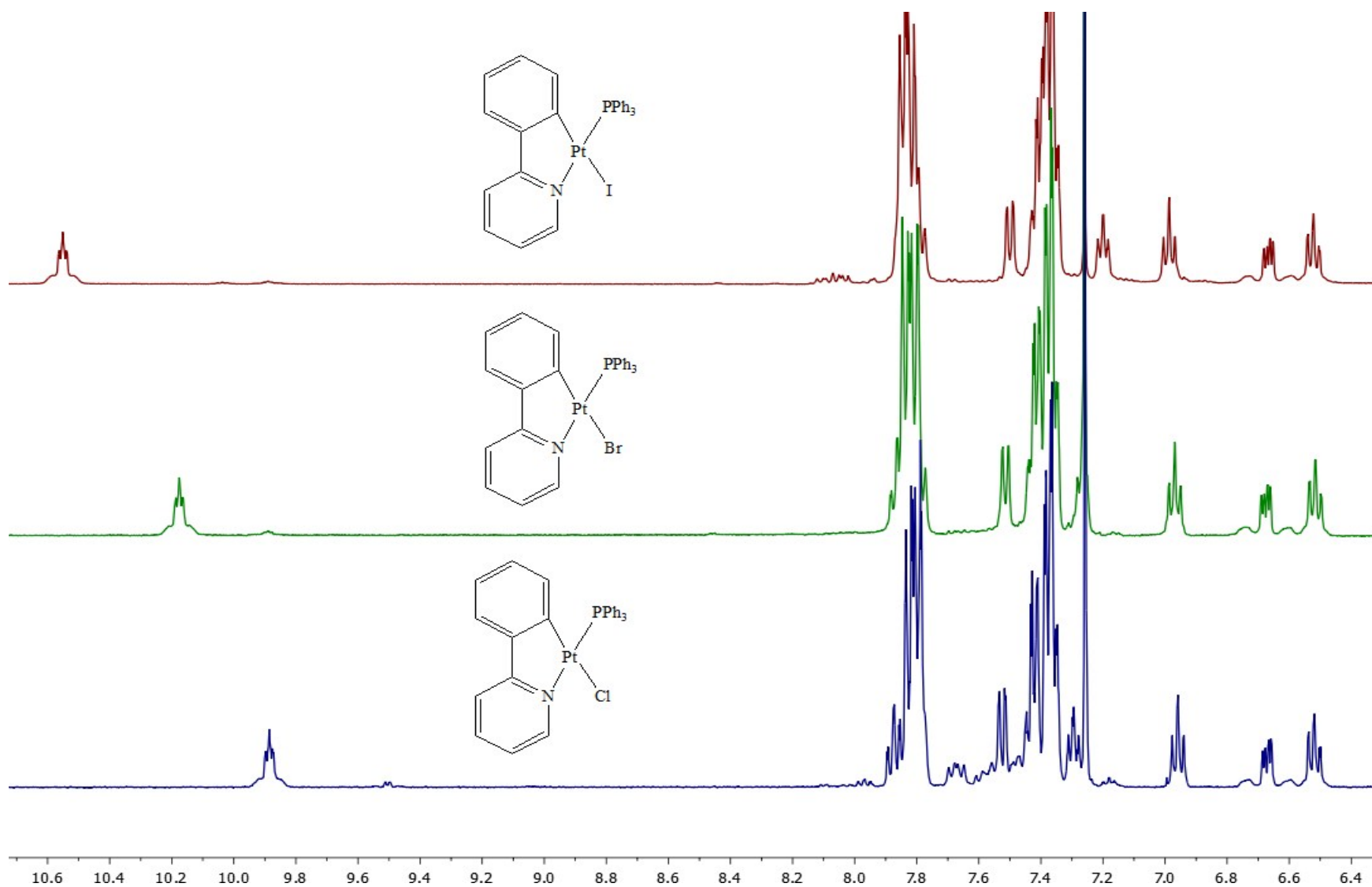


**Figure S9.**  $^1\text{H}$  NMR spectra of  $[\text{Pt}(\text{ppy})(\text{PPh}_3)\text{X}]$ ,  $\text{X} = \text{Cl}$ ,  $\text{Br}$  and  $\text{I}$ , in  $\text{CDCl}_3$ , illustrating the effect of the halide ligand on the chemical shift of hydrogen adjacent to the coordinated nitrogen atom.

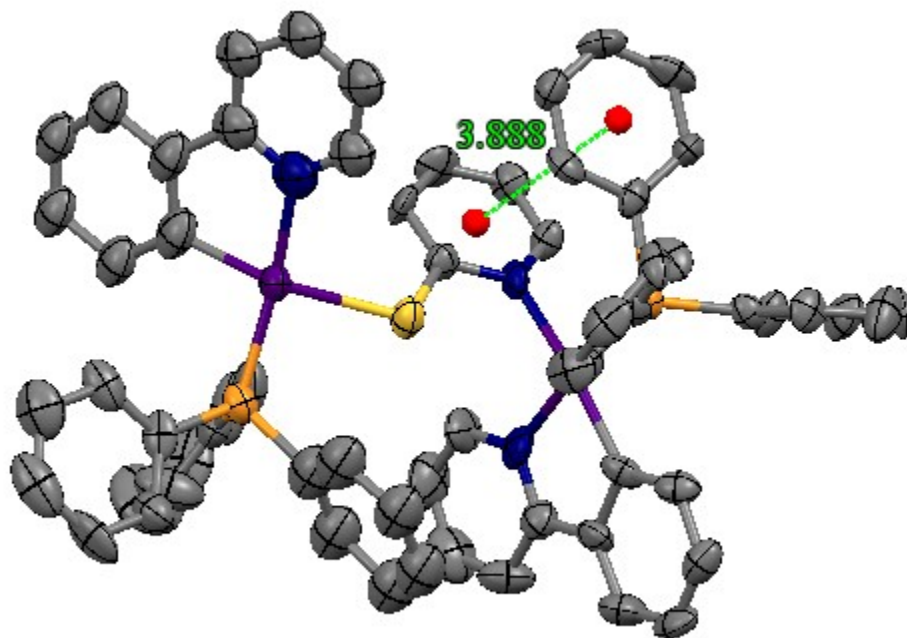


**Figure S10.** Weak intramolecular  $\pi \cdots \pi$  contact between the Spy and phenyl ring of PPh<sub>3</sub> in complex **3-PF<sub>6</sub>**.

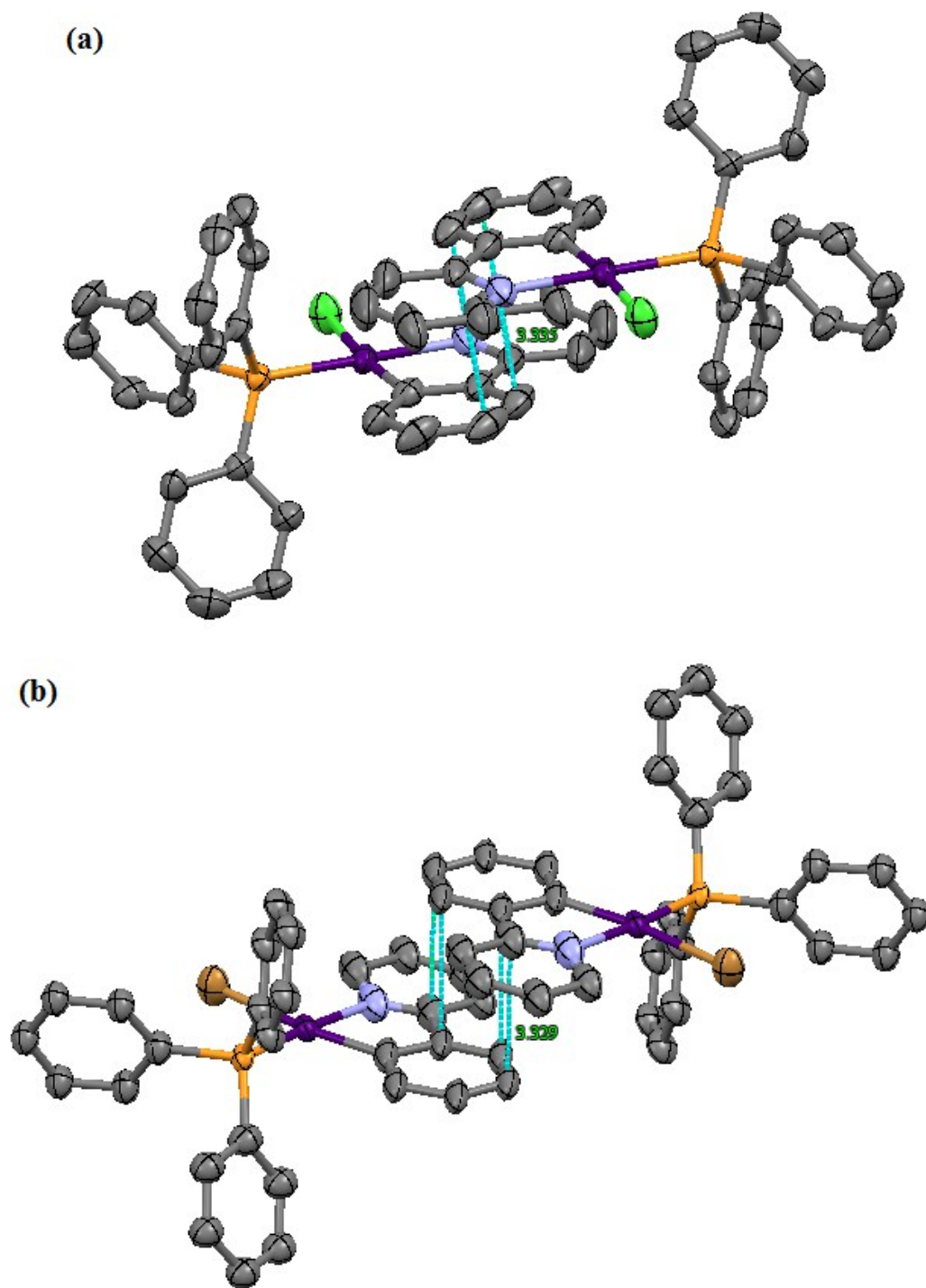


**Figure S11.** Crystal packing of complexes (a) **A** and (b) **2b** are displaying the intermolecular contacts. The supramolecular packing is formed by dimers supported by intermolecular  $\pi \cdots \pi$  interactions involving two ppy ligands.

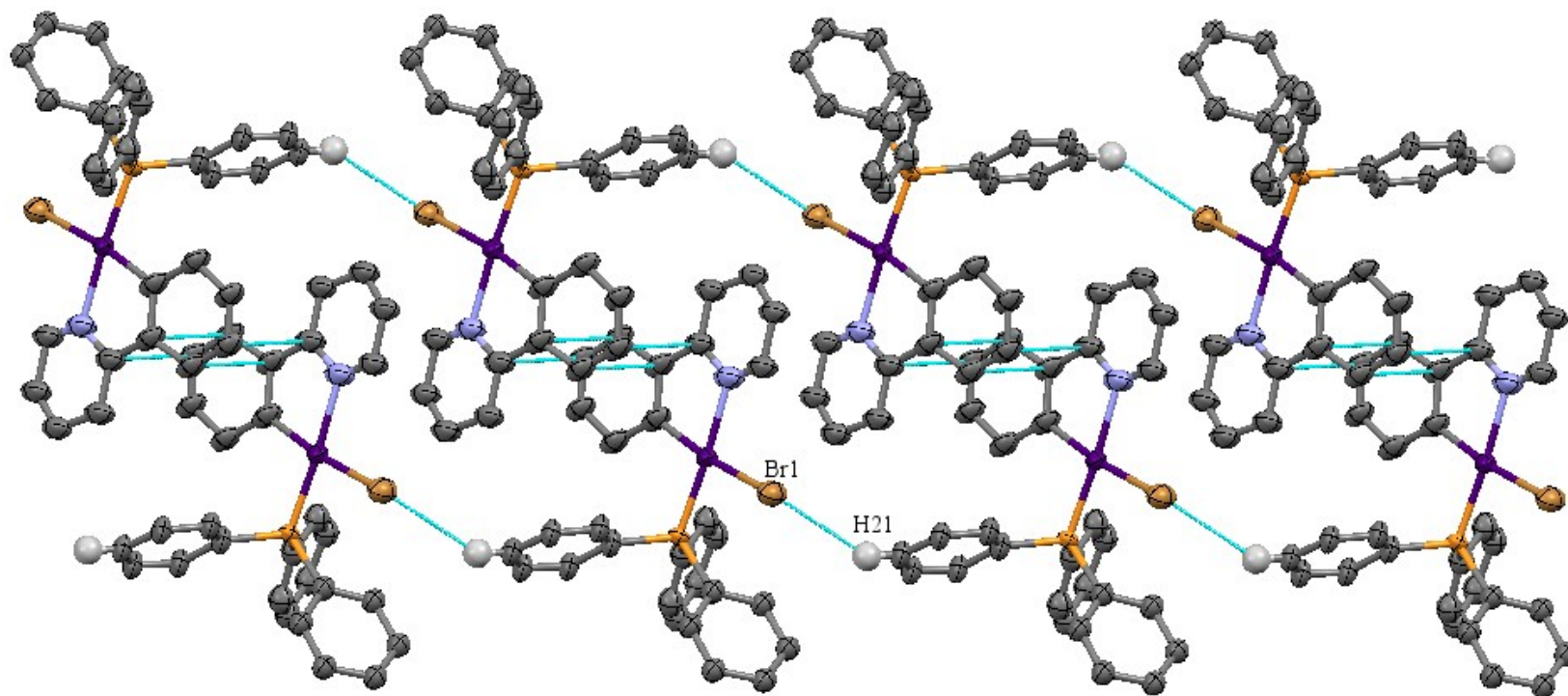


**Figure S12.** Partial view of the 2D-network of complex **2b** in the solid state. The hydrogen atoms are omitted for clarity, except for the hydrogen atoms being involved in Hydrogen bonding.

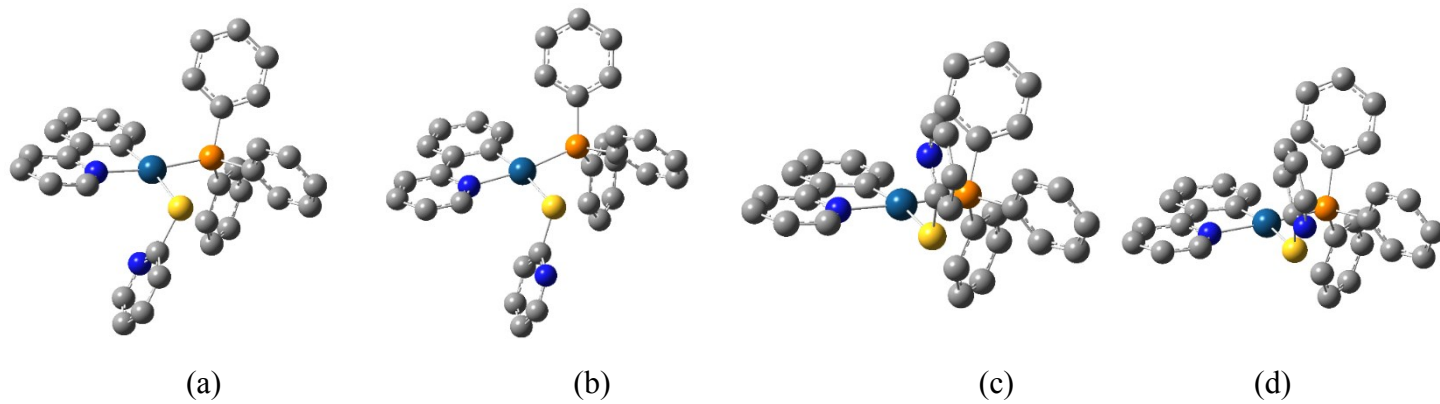


**Figure S13.** All possible geometries for complex **1a**.